Bioorganic & Medicinal Chemistry Letters 27 (2017) 4805–4811

Contents lists available at ScienceDirect

Bioorganic & Medicinal Chemistry Letters

journal homepage: www.elsevier.com/locate/bmcl

Highly potent and selective $Na_V1.7$ inhibitors for use as intravenous agents and chemical probes

R. Ian Storer [a,k,*], Andy Pike [b,k], Nigel A. Swain [a], Aristos J. Alexandrou [c], Bruce M. Bechle [e], David C. Blakemore [a], Alan D. Brown [a], Neil A. Castle [f], Matthew S. Corbett [e], Neil J. Flanagan [d], David Fengas [g], M. Scott Johnson [f], Lyn H. Jones [h], Brian E. Marron [f], C. Elizabeth Payne [c], David Printzenhoff [f], David J. Rawson [i], Colin R. Rose [e], Thomas Ryckmans [i], Jianmin Sun [e], Jonathan W. Theile [f], Rubben Torella [a], Elaine Tseng [j], Joseph S. Warmus [e]

[a] *Worldwide Medicinal Chemistry, Pfizer Ltd, The Portway, Granta Park, Cambridge CB21 6GS, UK*
[b] *Pharmacokinetics, Dynamics and Metabolism, Pfizer Ltd, The Portway, Granta Park, Cambridge CB21 6GS, UK*
[c] *Electrophysiology, Pfizer Ltd, The Portway, Granta Park, Cambridge CB21 6GS, UK*
[d] *Pharmaceutical Sciences, Pfizer Ltd, The Portway, Granta Park, Cambridge CB21 6GS, UK*
[e] *Worldwide Medicinal Chemistry, Pfizer Inc., Eastern Point Road, Groton, CT 06340, USA*
[f] *Icagen Inc, 4222 Emperor Blvd #350, Durham, NC 27703, USA*
[g] *Peakdale Molecular, Ltd, Discovery Park House, Ramsgate Road, Sandwich, Kent CT13 9ND, UK*
[h] *Worldwide Medicinal Chemistry, Pfizer Inc, 610 Main Street, Cambridge, MA 02139, USA*
[i] *Worldwide Medicinal Chemistry, Ramsgate Road, Sandwich, Kent CT13 9NJ, UK*
[j] *Pharmacokinetics, Dynamics and Metabolism, Pfizer Inc, Eastern Point Road, Groton, CT 06340, USA*

ARTICLE INFO

Article history:
Received 22 July 2017
Revised 17 September 2017
Accepted 27 September 2017
Available online 28 September 2017

Keywords:
Acid isostere
Ion channel
Pain
Voltage-gated

ABSTRACT

The discovery and selection of a highly potent and selective $Na_V1.7$ inhibitor PF-06456384, designed specifically for intravenous infusion, is disclosed. Extensive *in vitro* pharmacology and ADME profiling followed by *in vivo* preclinical PK and efficacy model data are discussed. A proposed protein–ligand binding mode for this compound is also provided to rationalise the high levels of potency and selectivity over inhibition of related sodium channels. To further support the proposed binding mode, potent conjugates are described which illustrate the potential for development of chemical probes to enable further target evaluation.

Voltage-gated sodium (Na_V) channels comprise a family of nine members $Na_V1.1$-$Na_V1.9$. They are members of the 6-TM ion channel sub-family that are structurally composed from a main transmembrane α-subunit of approximately 260 kDa with multiple lower molecular weight associated β-subunits.[1] Na_V channels have been established to play important roles in the control of neuronal excitability by regulating the threshold of firing and duration of inter-spike interval underlying the formation and propagation of action potentials.[2] Unselective sodium channel blockers are known and include established clinical agents (eg mexiletine **1**, lidocaine **2** and lamotrigine **3**) that have been used successfully to modulate neuronal firing patterns in a range of conditions including epilepsy and chronic pain (Fig. 1).[3,4] However, due to a lack of selectivity across the Na_V family, these drugs suffer narrow therapeutic indices over adverse effects due to inhibition of sodium channels in the brain (eg $Na_V1.1$, $Na_V1.2$) and heart (eg $Na_V1.5$).[5]

Abbreviations: ADME, absorption, distribution, metabolism and excretion; Cl_{int}, intrinsic clearance; Cl_p, plasma clearance; Cl_u, unbound clearance; DCM, dichloromethane; DHEP, dog hepatocytes; DLM, dog liver microsomes; DMAc, dimethylacetamide; DMF, dimethylformamide; DMSO, dimethyl sulfoxide; EP, manual electrophysiology; F, bioavailability; f_u, fraction unbound; HHEP, human hepatocytes; HLM, human liver microsomes; IC_{50}, half-maximum inhibitory concentration; IV, intravenous; lipE, lipophilic efficiency; OATP, organic anion-transporting polypeptide; PEG, polyethylene glycol; PK, pharmacokinetics; ppb, plasma protein binding; PX, PatchXpress® electrophysiology; RHEP, rat hepatocytes; RLM, rat liver microsomes; RRCK, Ralph Russ canine kidney cell line; SAR, structure activity relationship; SNAr, nucleophilic aromatic substitution; $T_{1/2}$, half-life; TEA, trimethylamine; TEMPO, (2,2,6,6-Tetramethylpiperidin-1-yl)oxyl; THF, tetrahydrofuran; TPSA, topological polar surface area; V_{ss}, apparent volume of distribution at steady state.

* Corresponding author.
E-mail address: ian.storer@astrazeneca.com (R.I. Storer).
[k] Current address: Astrazeneca, Darwin Building, 310 Cambridge Science Park, Milton Road, Cambridge CB4 0FZ, UK.

https://doi.org/10.1016/j.bmcl.2017.09.056
0960-894X/

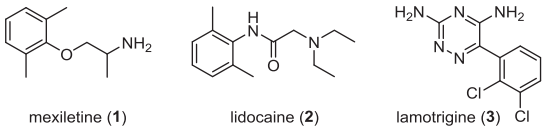

Fig. 1. pan-Na_V inhibitor drugs.

It is only in the last 10–15 years that a better understanding of which specific Na_V channels are likely to provide greatest therapeutic value has emerged. Human genetic data has pointed to a number of specific Na_V subtypes as playing a critical role in pain signal generation and transduction. Of these, $Na_V1.7$ has emerged as a particularly compelling target based on evidence of both gain-of and loss-of function mutations in the encoding SCN9A gene showing a strong association with pain and itch.[6–13] In particular, in 2006 it was reported that a loss-of-function mutation in this gene was responsible for a rare human genetic condition that manifests as a congenital insensitivity to all types of pain.[6] On this basis over the last decade there has been a significant interest in the discovery of subtype selective inhibitors of $Na_V1.7$.[14–19]

The design of subtype selective Na_V inhibitors remains a highly challenging prospect that is compounded by a lack of robust structural biology understanding of ion channel function and binding sites for functional modulation by small molecules. The established unselective pan-Na_V inhibitors are believed to bind to an intracellular site within the channel pore. However, design of subfamily selectivity at this binding site has proved challenging, likely owing to high sequence homology within this region across the Na_V subfamily.[20,21]

Despite these challenges we were able to pioneer a series of acidic heterocyclic sulfonamide $Na_V1.7$ inhibitors that exhibited good levels of potency and intra-family selectivity, culminating in the delivery of an oral clinical candidate PF-05089771 (**4**) (Fig. 2).[22,23] Also, via application of site directed mutagenesis, the Na_V subtype selectivity inherent to this series was rationalised to result from binding to a novel site in the domain IV voltage sensor of the alpha subunit.[24] Further supporting evidence was subsequently provided by an X-ray co-crystal structure of a Pfizer patent compound by Genentech and Xenon[25] who, along with several other companies, had also opted to pursue acidic sulfonamide inhibitors.[26–29]

As an alternative therapeutic modality a program was initiated to design a compound for intravenous (IV) infusion to treat acute traumatic, perioperative pain or postoperative pruritus in a clinical setting where oral dosing is not convenient. The product concept included targeting rapid clearance to minimise any residual on or off target drug effects following the end of infusion. This required a compound with high potency, to at least partially offset the high clearance and minimise dose requirements, as well as good solubility in order to be compatible with IV formulations and minimise infusion volumes.

To design a suitable intravenous (IV) infusion compound, SAR knowledge gained from our oral $Na_V1.7$ program was incorporated to deliver optimal $Na_V1.7$ inhibition potency and solubility, ultimately resulting in PF-06456384 (**5**) (Fig. 2).[30]

Some key SAR which guided the design that led to compound **5** is illustrated in Table 1. A strategy that comprised combining the most lipophilic efficient (lipE)[31] fragments was adopted in order to deliver optimal potency and selectivity. Accordingly, it had previously been observed that compounds containing a polar 1,2,4-thiadiazole sulfonamide acidic headgroup in combination with a nitrile substituted core ring (compounds **5**–**8**, **13**) provided the most lipophilic efficient and intra-Na_V selective compounds.[32] However, despite the potency and selectivity advantages, for the oral program this combination had often led to poor *in vivo*

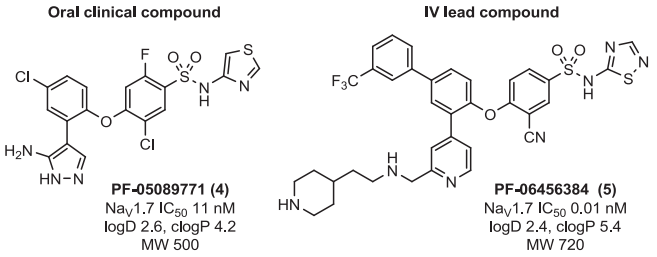

Fig. 2. Oral candidate[22] and IV lead compounds.

intestinal absorption due to low permeability, likely driven by high topological polar surface area (TPSA >150 Å^2) and acidity of the heterocyclic sulfonamide. However, in the case of IV administration intestinal permeability was no longer of relevance. Also it had previously been established that scope for further variation of either the amino heterocycle or core substituents was relatively limited.[32] However, several other key combinations were also known to be reasonably efficient such as 4-thiazole (**4**, **11**) or 1,3,4-thiadiazole (**9**–**10**, **12**) in combination with a F,Cl di-substituted core ring. In contrast, broader variation of substitution around the left hand ring of the diaryl ether group (as drawn) and of the pendant *ortho*-ring could be readily tolerated, providing opportunity for gains in potency and lipE plus the introduction of groups to specifically modulate the bulk physical properties of the molecules such as polar and ionisable groups.

Beginning with zwitterionic compound **6** as a reasonably potent ($Na_V1.7$ IC_{50} 8.5 nM) and lipophilic efficient (lipE 4.5) lead, various modifications were combined to maximise ligand potency. Firstly, it was observed that the primary benzylic amine in compound **6** could be replaced with either secondary (**7**) or tertiary (**8**) amines whilst maintaining good levels of lipE (4.2–4.5) and therefore modulating potency in line with lipophilicity. Secondly, by comparing compounds **9** (lipE 2.6) and **10** (lipE 4.3), a notable increase in ΔlipE >1.0 could be obtained by introduction of a nitrogen into the ortho ring, rendering this a 2-substituted pyridine (**10**). By cross-comparing a selection of favoured core/amino heterocycle combinations (compounds **8**–**11**) it appeared that the 1,2,4-thiadiazole in combination with a nitrile core remained the most lipophilic efficient as observed in the oral drug discovery campaign. Thirdly, a *meta*-CF_3 substituted phenyl ring was introduced para to the diaryl ether linkage. Previous experience had shown this group to be tolerated, essentially driving increased potency through additional lipophilicity. As a result, the ortho 2-pyridine lipE enhancing group was combined with the *meta*-CF_3 system to maximise potency in compounds **12** ($Na_V1.7$ IC_{50} 1.5 nM, lipE 3.7) and **13** ($Na_V1.7$ PX IC_{50} 0.5 nM, lipE 5.1). However, despite the good levels of potency, these compounds were poorly soluble in the desired IV formulation pH 3-8 range (compound **12** solubility in aqueous buffer: pH 3.0 = 6 μg/mL, pHs 4.2/5.1/7.2 = <0.5 μg/mL).

Therefore, based on the earlier SAR observed for compound **7**, a dibasic amino-substituted piperidine group was introduced to provide compound **5**. The rationale for this was primarily to provide an overall weakly basic compound with the other two ionisable centres existing as a zwitterion at neutral pH, thereby maximising solubility and compatibility with IV formulations, whilst simultaneously maintaining excellent potency. Initial automated electrophysiology profiling of compound **5** on a PatchXpress® (PX) platform gave $Na_V1.7$ PX IC_{50} = 0.58 nM (lipE 3.8). Although very potent, this was weaker than anticipated based on previous SAR, which had suggested that this compound should have a lipE >5 which would in turn result in a $Na_V1.7$ IC_{50} < 100 pM. Further investigation via conventional single cell patch clamp

Table 1
Selected SAR used in the design of compound **5**.

No.	Structure	$Na_V1.7$ PX IC_{50} (nM)[a]	clogP	lipE[c]
6	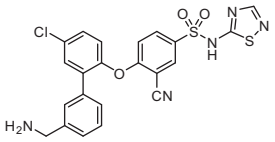	8.5	3.6	4.5
7	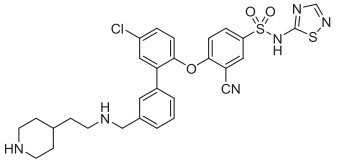	0.70	4.8	4.4
8	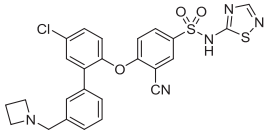	1.6	4.6	4.2
9	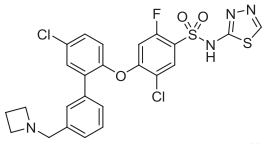	8.6	5.5	2.6
10	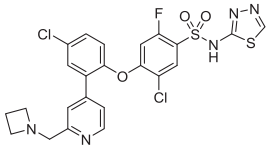	4.8	4.0	4.3
11	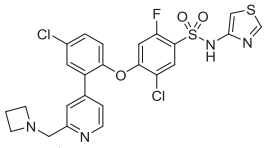	13.2	4.0	3.9
12	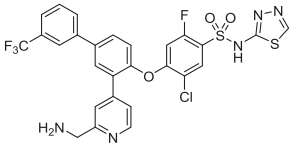	1.5	5.1	3.7
13	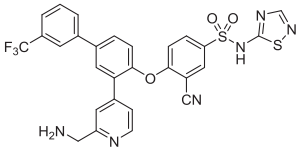	0.50 (EP 0.1)[b]	4.2	5.1 (5.8)
5	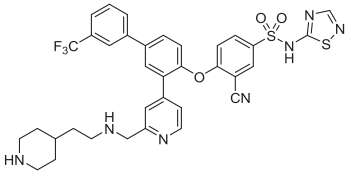	0.58 (EP 0.01)[b]	5.4	3.8 (5.6)

[a] PX = PatchXpress® electrophysiology.
[b] EP = Conventional Patch Clamp electrophysiology.
[c] lipE = $-\log IC_{50}$ − clogP. IC_{50} values are based on the average of >2 determinations (see SI for details).

electrophysiology (EP) showed that both compounds **13** and **5** were indeed more potent (EP IC_{50}s 100 pM and 10 pM respectively) in line with the anticipated lipE of around 5.5. Further investigation suggested that the PatchXpress® platform struggled to accurately determine potent (<1 nM) IC_{50}s due to slow equilibration kinetics, therefore requiring longer duration recordings that were only possible by conventional EP (see SI section for details of the electrophysiology protocols used and for a more full discussion of protocols see Ref. 22).

Recently Genentech and Xenon reported a $Na_V1.7$ X-ray co-crystal structure,[25] in the presence of Pfizer compound PF-05196233 (**GX-936**) from the same chemotype as compound **5** (Fig. 3).[23] To rationalise the extreme potency, compound **5** was docked using this published structure as a reference protein.

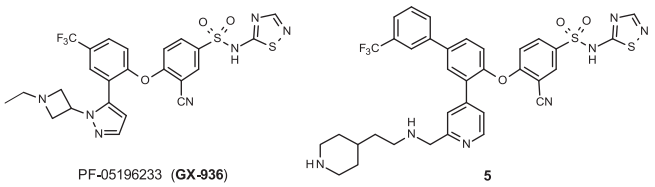

Fig 3. Structures of compound GX-936 & IV lead compound **5**.

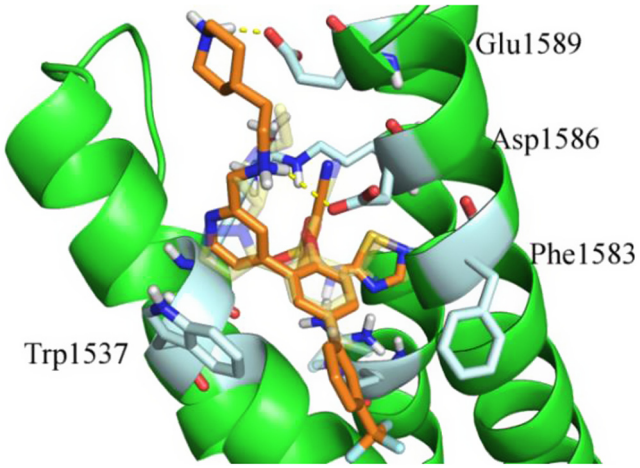

Fig. 4. Docking pose of compound **5** (orange), overlaid with X-ray pose of GX936 (transparent yellow). The described new set of interactions with Phe1583, Trp1537, Asp1586 and Glu1589 is shown by yellow dashes.

Table 2
$Na_V1.7$ activities for amide conjugated derivatives.

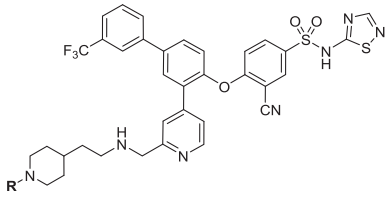

No.	R Group	$Na_V1.7$ IC_{50} (nM)	$Na_V1.5$ IC_{50} (nM)
14		<4[a]	nt
15	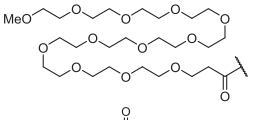	<10[a]	>3000[a]
16	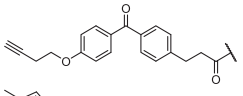	0.10[b]	nt
17	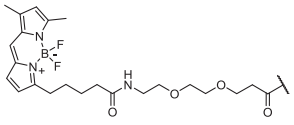	0.12[b]	nt

[a] PatchXpress® electrophysiology.
[b] Conventional Patch Clamp electrophysiology.

Compound **5** (orange) is predicted by docking to bind in a similar manner and orientation to GX-936 (yellow), making consistent interactions between the acidic sulfonamide and arginine residues in the binding site (Fig. 4).

However, there are some interesting differences that can be highlighted from this analysis which likely account for the excellent potency of compound **5**: i) the additional *meta*-trifluoromethyl substituted aromatic ring in compound **5** is predicted to embed into the membrane, flanked by two aromatic residues (Phe1583 and Trp1537) which can both make π-π stacking interactions; ii) the pyridine ring in compound **5** can π-stack with Trp1537 in an analogous manner to the pyrazole in GX-936; iii) the additional flexibility of the benzylamine in compound **5** relative to the rigid azetidine in GX-936 allows for a more optimal salt bridge interaction with Asp1586 and; iv) the basic nitrogen of the piperidine in compound **5** can form an additional interaction with Glu1589 at the top of the voltage-sensor domain (VSD). Taken together, these additional interactions likely rationalise why compound **5** confers such high levels of potency.

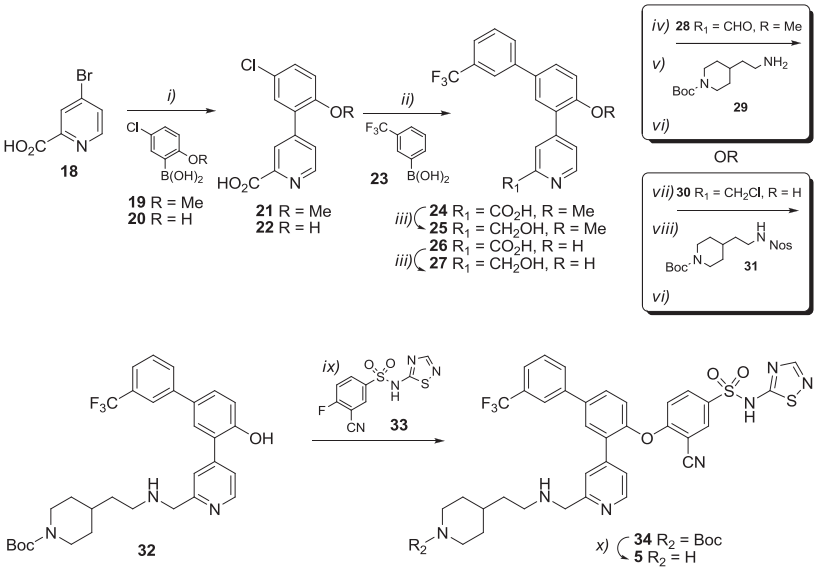

Scheme 1. Reagents and conditions: i) **19** or **20**, $Pd(PPh_3)_4$, Na_2CO_3, dioxane/H_2O. ii) **23**, $Pd(OAc)_2$, s-SPhos, K_2CO_3, H_2O. iii) BH_3-THF, THF. iv) TEMPO, NaClO, DCM (95%). v) **29**, $NaBH_4$, $MgSO_4$, DCM (87%). vi) dodecane thiolate, NaOH, DMSO. vii) $POCl_3$, DMF, DCM. viii) **30**, NaH, DMAc (65%). ix) **33**, K_2CO_3, DMSO (80%). x) HCl, MeOH (76%).

Interestingly, the proposed positioning of the piperidine at the mouth of the pocket pointing into solvent suggests that this might be a suitable handle from which further groups could be appended without significantly impacting the binding energy due to exiting the extracellular binding site. It was decided to explore this hypothesis further with a view to being able to potentially exploit this feature for the introduction of pharmacokinetic (PK) modulating conjugations or provision of functional probes. To initially investigate whether amide attachment and conjugate linkers could be tolerated acyl capped (**14**) and PEG-12 amide (**15**) compounds were synthesised (Table 2). Pleasingly, both of these modifications maintained good potency, giving complete channel block at low nM levels (no accurate IC_{50} was determined in these cases). Furthermore PEG-12 amide (**15**) was also tested for activity at $Na_V1.5$ for which it showed no significant activity, thereby suggesting that the high levels of selectivity inherent to the headgroup had been maintained. To further build on this initial result, a BODIPY®FL (**16**) fluorescent conjugate,[37] and benzophenone photoprobe (**17**) compound (potentially useful for binding or target engagement studies,[35,36] or for determination of the $Na_V1.7$ interactome) were synthesised.[38,39] Interestingly, these conjugates all maintained excellent sub-nanomolar levels of $Na_V1.7$ potency (Table 2). The apparently flat $Na_V1.7$ IC_{50} SAR for the conjugate groups supports the initial proposal that the piperidine moiety on the headgroup offers a trajectory out of the binding site, thereby positioning the conjugate groups into solvent leading to them not significantly impacting binding affinity.

In order to prepare compound **5** and derivatives, a concise convergent synthetic route via phenol intermediate **32** was developed allowing late stage S_NAr coupling with fluorophenyl **33** (Scheme 1). The biphenyl pyridyl in compound **32** was installed using sequential Suzuki-Miyaura reactions. The couplings of the 4-bromonicotinic acid **18** with either methoxy-phenylboronic acid **19** or phenolboronic acid **20**, catalysed by tetrakis(triphenylphosphine)-palladium(0), proceeded smoothly, but the subsequent Suzuki-Miyaura coupling reactions with boronic acid **23** proved to be low yielding in both cases using standard catalysts. However, application of Buchwald's water soluble SPhos proved superior, providing high yields of either the methoxy acid **24** or phenol acid **26**.[40] Furthermore, use of this catalyst also enabled the two couplings to be completed in one-pot by simply adding the second boronic acid to the reaction after the first coupling was deemed complete by HPLC.

To incorporate the requisite amino-piperidine to access compound **32**, a reductive amination with primary amine **29** could be carried out. However, it proved necessary to have the phenol masked as the methyl ether **25** in order to successfully prosecute this reductive amination. Alternatively a Fukuyama amine synthesis using nosyl protected amine **31** could be applied as the key bond forming reaction.[41] In this case, the free phenol **27** could be successfully reacted to provide phenol **32** which was subsequently coupled via S_NAr to give compound **34** followed by deprotection to lead compound **5** (Scheme 1).

Having identified compound **5** as a highly potent lead compound, extensive selectivity profiling was carried out across Na_V channel human subtypes and relevant orthologues using conventional EP. Pleasingly, compound **5** proved to be exquisitely selective over sodium channels that are associated with cardiovascular and CNS activities (>300× selective over all other human Na_Vs) as shown in Table 3. Further wide ligand secondary pharmacology assessment across a broad panel of target classes was also carried out (see SI section 6 for table of this data). All pharmacologies tested in this panel also showed >1000-fold weaker activity than the primary $Na_V1.7$ IC_{50}.

Solubility assessment showed compound **5** to have very good solubility in aqueous buffer of >900 μg/mL across the relevant pH 3–7 range which enabled formulations to solutions of 10 mg/mL at pH 5–6.

Table 3
Physical properties, *in vitro* pharmacology and ADME data for compound **5**.

Property	Compound **5**
Physicochemical properties	
Molecular weight (Da)	719.8
clogP	5.37
logD ($pH_{7.4}$)	2.37
pK_a (acid)	2.6
pK_a (base)	9.3, 6.6
TPSA (Å^2)	178
Solubility at pH 3.2 (μg/mL)	>906
Solubility at pH 4.2 (μg/mL)	>1172
Solubility at pH 5.5 (μg/mL)	>1835
Solubility at pH 7.1 (μg/mL)	>2573
Na_V Pharmacology[a]	
$hNa_V1.1$ IC_{50} (nM)	314
$hNa_V1.2$ IC_{50} (nM)	3
$hNa_V1.3$ IC_{50} (nM)	6438
$hNa_V1.4$ IC_{50} (nM)	1451
$hNa_V1.5$ IC_{50} (nM)	2592
$hNa_V1.6$ IC_{50} (nM)	5.8
$hNa_V1.7$ IC_{50} (nM)	0.01
$hNa_V1.8$ IC_{50} (nM)	26000
$mNa_V1.7$ IC_{50} (nM)	<0.1
$rNa_V1.7$ IC_{50} (nM)	75
ADME in vitro profile	
RRCK (×10^{-6} cm/s)	0.62
HLM, Clint (μL/min/mg)	<8.0
RLM, Clint (μL/min/mg)	<14.1
DLM, Clint (μL/min/mg)	<18.1
MLM, Clint (μL/min/mg)	ND
HHEP, Clint (μL/min/10^6 cells)	6.5
RHEP, Clint (μL/min/10^6 cells)	<6.0
DHEP, Clint (μL/min/10^6 cells)	<6.0
MHEP, Clint (μL/min/10^6 cells)	<3.0
Human microsomal binding	0.0012
hppb (fraction unbound)	0.00497
rppb (fraction unbound)	0.00275
dppb (fraction unbound)	0.00374
mppb (fraction unbound)	0.00281
Human blood:plasma	0.573
Rat blood:plasma	0.467
Dog blood:plasma	0.447
Mouse blood:plasma	0.543
CYP inhibition IC_{50}	
CYP1A2 (μM)	>30
CYP2C8 (μM)	6.17
CYP2C9 (μM)	3.75
CYP2C19 (μM)	1.32
CYP2D6 (μM)	8.83
CYP3A4 (μM)	1.15
OATP cell uptake	
OATP1B1 (transfected/wild type)	3.9
OATP1B3 (transfected/wild type)	3.4
OATP2B1 (transfected/wild type)	3.6

[a] See SI for details of electrophysiology assay protocols.

In vitro ADME profiling of compound **5** was carried out across a panel of assays. This included metabolic stability assays and showed low Cl_{int} in both microsomes and hepatocytes from mouse, rat, dog and human. This finding is consistent with low metabolic clearance of Compound **5**, albeit the low microsomal f_u may be confounding this measurement. However, the rate limiting clearance step of the oral clinical compound PF-5089771 (**4**) and the related series was usually active hepatic uptake via organic anion transporting polypeptides (OATPs).[33]

Given the significant changes in physicochemical properties between compound **5** and the oral series, including increased

Table 4
Preclinical *in vivo* IV PK.

Species/Property	Compound **5**
Mouse	
Cl_p (mL/min/kg)	36.5
Cl_u (mL/min/kg)	12989
Cl_b (mL/min/kg) [b]	67.2
$T_{1/2}$ (h)	0.66
V_{ss} (L/kg)	0.54
Rat	
Cl_p (mL/min/kg)	83.1 (59.8[a])
Cl_u (mL/min/kg)	30218
Cl_b (mL/min/kg) [b]	178
$T_{1/2}$ (h)	0.21
V_{ss} (L/kg)	0.59
Biliary (mL/min/kg)	44.0
Renal (mL/min/kg)	0.0322
Dog	
Cl_p (mL/min/kg)	17.8
Cl_u (mL/min/kg)	4759
Cl_b (mL/min/kg)[b]	39.8
$T_{1/2}$ (h) α/β	0.057/5.9
V_{ss} (L/kg)	0.46
Renal (mL/min/kg)	0.0012

[a] Cl_p value from bile duct cannulated rat study.
[b] Cl_b calculated from plasma clearance and measured blood:plasma.

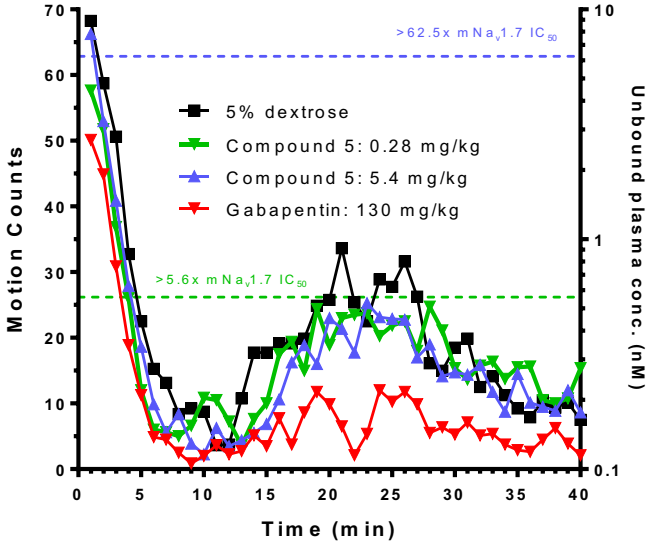

Fig. 5. Mouse formalin efficacy model. To achieve steady state plasma concentrations, IV infusion of compound commenced 90 min prior to formalin injection (0 min on graph) and continued throughout the testing phase. Dashed lines indicate unbound plasma concentration measured at the end of the experiment. However, these are expected to be representative of the entire testing period.

molecular weight and the addition of the pendent dibasic sidechain, it was unclear if this would still be the case. As a result uptake of compound **5** in OATP expressing cell lines vs wild type was assessed. Despite the altered physicochemistry, these suggested that compound **5** was indeed an OATP substrate (Table 3).

Compound **5** was subsequently profiled in preclinical *in vivo* pharmacokinetic studies (Table 4). It exhibited high total blood clearance, close to or exceeding liver blood flow, and very high unbound clearance in all species. In bile duct cannulated rats, 74% of the dose was recovered unchanged in bile, supporting active uptake and excretion as a major clearance mechanism of this compound in this species. Renal clearance was not significant in either rat or dog. The volume of distribution approximated body water in all species. However, in dog an extended β phase of elimination was observed which may indicate more extensive distribution of a fraction of the dose. Taken together this extensive profiling suggested suitability of compound **5** for progression to *in vivo* efficacy studies as a potential candidate drug.

Lead compound **5** was therefore tested for analgesic efficacy in a mouse formalin model following continuous IV infusion. Published data in $Na_V1.7$ knockout mice suggests these animals recapitulate the human phenotype, showing congenital insensitivity to all pain and minimal response in the formalin test, indicating this model to be relevant to $Na_V1.7$ pharmacology.[11] Compound **5** was tested for analgesic efficacy in a wild type mouse formalin model with continuous infusion. However, despite achieving unbound plasma concentration of ≥60× the mouse $Na_V1.7$ IC_{50}, there was no significant effect of the compound in this model relative to Gabapentin as the positive control (Fig. 5).

This lack of preclinical efficacy in the mouse formalin model was unexpected given the published $Na_V1.7$ mouse knock out data.[11] Ultimately this data contributed to compound **5** being discontinued as a potential intravenous drug candidate for pain. However, the exquisite potency and selectivity coupled with the opportunity to exploit the free piperidine for the synthesis of probe derivatives, suggest that these compounds could potentially be used as tools to enable further work to better understand target engagement and how selective chemical modulation of $Na_V1.7$ might translate into pain efficacy.[34–36]

In summary, a highly potent and subtype selective $Na_V1.7$ inhibitor PF-06456384 (**5**) was designed and synthesised for application as an IV infusion agent. The compound was extensively profiled *in vitro* and taken into *in vivo* PK studies which suggested a profile commensurate with the intended application. However compound **5** ultimately showed a lack of preclinical efficacy in a mouse formalin pain model and was not progressed further. Nonetheless, compound **5** constitutes an exceptionally potent and selective tool. Aligned with this, potent conjugated probes of compound **5** were prepared to illustrate the potential to support further *in vitro* and *in vivo* evaluation of the translation of $Na_V1.7$ inhibition to the treatment of pain.

Acknowledgments

We thank Mark Chapman, Zhixin Lin and Ian Witton for generation of automated patch clamp data. Also we thank Rosemarie Roeloffs and WuXi Pharmatech for generation of *in vivo* model pain efficacy data. We also thank Simon Armitage, Bruce Brown, Stephanie Dupuy, Steve Reister and Peakdale Molecular for compound analogue synthesis.

A. Supplementary data

Supplementary data associated with this article can be found, in the online version, at https://doi.org/10.1016/j.bmcl.2017.09.056.

References

1. Bagal SK, Brown AD, Cox PJ, et al. *J Med Chem*. 2013;56(3):593–624.
2. Wood JN, Boorman J. *Curr Top Med Chem*. 2005;5(6):529–537.
3. Dib-Hajj SD, Yang Y, Black JA, Waxman SG. *Nat Rev Neurosci*. 2013;14(1):49–62.
4. Lampert A, Eberhardt M, Waxman SG. *Handb Exp Pharmacol*. 2014;221:91–110 (Voltage Gated Sodium Channels).
5. Eijkelkamp N, Linley John E, Baker Mark D, et al. *Brain*. 2012;135(Pt 9):2585–2612.
6. Cox JJ, Reimann F, Nicholas AK, et al. *Nature*. 2006;444(7121):894–898.
7. Fertleman CR, Baker MD, Parker KA, et al. *Neuron*. 2006;52(5):767–774.
8. Yang Y, Wang Y, Li S, et al. *J Med Genet*. 2004;41(3):171–174.
9. Snyder LM, Ross SE, Belfer I. *Pain*. 2014;155(9):1677–1678.
10. Devigili G, Eleopra R, Pierro T, et al. *Pain*. 2014;155(9):1702–1707.

11. Gingras J, Smith S, Matson DJ, et al. *PLoS ONE*. 2014;9(9):14. e105895/1–e105895/14.
12. Drenth JPH, te Morsche RHM, Guillet G, Taieb A, Kirby RL, Jansen JBMJ. *J Invest Dermatol*. 2005;124(6):1333–1338.
13. Goldberg YP, MacFarlane J, MacDonald ML, et al. *Clin Genet*. 2007;71(4):311–319.
14. Nardi A, Damann N, Hertrampf T, Kless A. *ChemMedChem*. 2012;7(10):1712–1740.
15. Bagal SK, Chapman ML, Marron BE, Prime R, Storer RI, Swain NA. *Bioorg Med Chem Lett*. 2014;24(16):3690–3699.
16. de Lera RM, Kraus RL. *J Med Chem*. 2015;58(18):7093–7118.
17. King GF, Vetter I. *ACS Chem Neurosci*. 2014;5(9):749–751.
18. Sun S, Cohen CJ, Dehnhardt CM. *Pharm Pat Anal*. 2014;3(5):509–521.
19. England S, Rawson D. *Future Med Chem*. 2010;2(5):775–790.
20. England S, de Groot MJ. *Br J Pharmacol*. 2009;158(6):1413–1425.
21. England S. *Expert Opin Invest Drugs*. 2008;17(12):1849–1864.
22. Alexandrou AJ, Brown AR, Turner J, et al. *PLoS ONE*. 2016;11(4). e0152405/1–22.
23. Beaudoin S, Laufersweiler MC, Markworth CJ, et al., WO2010079443; 2010.
24. McCormack K, Santos S, Chapman ML, et al. *Proc Natl Acad Sci USA*. 2013;110(29):E2724–E2732.
25. Ahuja S, Mukund S, Deng L, et al. *Science*. 2015;350(6267):1491.
26. Focken T, Liu S, Chahal N, et al. *ACS Med Chem Lett*. 2016;7(3):277–282.
27. Sun S, Jia Q, Zenova AY, et al. *Bioorg Med Chem Lett*. 2014;24(18):4397–4401.
28. Marx IE, Dineen TA, Able J, et al. *ACS Med Chem Lett*. 2016;7:1062–1067.
29. DiMauro EF, Altmann S, Berry LM, et al. *J Med Chem*. 2016;59(17):7818–7839.
30. Swain NA, Brown AD, Jones LH, et al., WO2015181797; 2015.
31. Ryckmans T, Edwards MP, Horne VA, et al. *Bioorg Med Chem Lett*. 2009;19(15):4406–4409.
32. Swain NA, Beaudoin S, Bechle BM, et al. *J Med Chem*. 2017;60(16):7029–7042.
33. Lavis LD, Raines RT. *ACS Chem Biol*. 2008;3(3):142–155.
34. Bunnage ME, Gilbert AM, Jones LH, Hett EC. *Nat Chem Biol*. 2015;11(6):368–372.
35. Bunnage ME, Chekler ELP, Jones LH. *Nat Chem Biol*. 2013;9(4):195–199.
36. Kolb HC, Finn MG, Sharpless KB. *Angew Chem Int Ed*. 2001;40(11):2004–2021.
37. Wildburger NC, Ali SR, Hsu W-CJ, et al. *Mol Cell Proteomics*. 2015;14(5):1288–1300.
38. Anderson KW, Buchwald SL. *Angew Chem Int Ed*. 2005;44(38):6173–6177.
39. Kan T, Fukuyama T. *Chem Commun*. 2004;4:353–359.
40. Jones HM, Butt RP, Webster RW, et al. *Clin Pharmacokinet*. 2016;55(7):875–887.
41. Morgan P, Van Der Graaf PH, Arrowsmith J, et al. *Drug Discovery Today*. 2012;17(9–10):419–424.